

Modified spin-wave theory for the $S = 1$ frustrated antiferromagnetic Heisenberg chain

G.M. Rocha-Filho^{1,a}, A.S.T. Pires¹, and M.E. Gouvêa²

¹ Dept. de Física, ICEx, Universidade Federal de Minas Gerais, Av. Antônio Carlos 6627, Pampulha, 31270-901 Belo Horizonte, Brazil

² Centro Federal de Educação Tecnológica de Minas Gerais, Brazil

Received 5 October 2006 / Received in final form 20 December 2006

Published online 21 March 2007 – © EDP Sciences, Società Italiana di Fisica, Springer-Verlag 2007

Abstract. We study the one-dimensional isotropic spin-1 Heisenberg magnet with antiferromagnetic nearest-neighbor (nn) and next-nearest-neighbor (nnn) interactions by using the modified spin wave theory (MSWT). The ground state energy and the singlet-triplet energy gap are obtained for several values of j , defined as the ratio of the nnn interaction constant to the nn one. We also compare two different ways of implementing the MSWT currently found in the literature, and show that, despite the remarkable differences between the equations to be solved in each procedure, the results given by both are equivalent, except for the predicted value of the j_{max} , the maximum value of j accessible in each treatment. Here, we suggest that j_{max} is related to the disorder point of the first kind. Our results show that the ground state and the gap energies increase with j , for $j \leq j_{max}$, in accordance to previous numerical results.

PACS. 75.10.Jm Quantized spin models – 75.10.Pq Spin chain models – 75.30.Ds Spin waves – 75.50.Ee Antiferromagnetics

1 Introduction

In the last two decades, the physics of low dimensional magnets has continuously revealed many interesting and unexpected behavior stimulating a great number of theoretical, numerical, and experimental studies in the area. Among the systems that have deserved attention for their rich behavior are those with frustration which, many times, cannot be treated by conventional techniques. Concerning antiferromagnetic systems, our interest in this work, frustration tends to suppress antiferromagnetic correlations and, thus, the tendency towards Néel order. Therefore, the ground state of classical systems is of the Néel type only for small frustration; as the frustration is enhanced, the ground state exhibits an helical ordered state. In quantum systems, the interplay of frustration and quantum fluctuations may lead to a spin-liquid state or to some kind of spontaneous symmetry breaking.

The Heisenberg isotropic quantum spin chain with antiferromagnetic interactions between nearest (nn) and next-nearest neighbors (nnn) is one of the simplest quantum frustrated systems and, therefore, it is of prime importance. The model is described by the Hamiltonian

$$H = J_1 \sum_l \mathbf{S}_l \cdot \mathbf{S}_{l+1} + J_2 \sum_l \mathbf{S}_l \cdot \mathbf{S}_{l+2}, \quad (1)$$

where \mathbf{S}_l is a spin- S operator at site l , J_1 are J_2 are, respectively, the antiferromagnetic nn and nnn coupling constants. Hereafter, we will use $j = J_2/J_1$. It is now very well known that, in the limit of no frustration ($j = 0$), there is a fundamental difference between half-integer and integer spin chains; the so-called Haldane's conjecture [1]. For integer spin values, the model exhibits a non-magnetic singlet ground state well separated from the first excited triplet state by an energy gap Δ , whereas the excitation spectrum is gapless for half-odd-integer spin values.

Therefore, it is natural to expect different behavior for frustrated chains involving integer or half-odd-integer spins. The case of half-integer spin chains has been extensively studied and is by now very well understood [2]: the ground state is in the spin-fluid phase or in the dimer-phase [3,4] depending on whether j is smaller or larger than a critical value $j_c \approx 0.241$ [5,6]. Frustrated isotropic Heisenberg chains with integer spin have also attracted considerable interest. The ground state properties of the spin-1 frustrated chain were numerically investigated by Tonegawa et al. [7] and the phase diagram of this model has been the subject of many numerical and theoretical works. In the range of j -values investigated by Tonegawa et al. [7], it was found that the ground state energy and the singlet-triplet gap increase with j , at least for $j < 0.40$. The existence of a gap Δ for any value of j is predicted by field theoretical studies [8,9] but its behavior as a

^a e-mail: gmrocha@fisica.ufmg.br

function of j is not a monotonically increasing function, as shown in references [10, 11]. Using a variational ansatz starting from valence bond states and the density-matrix renormalization group, Kolezhuk et al. [12] explained the phase diagram of the model as follows: there is a disorder point at $j_D = 0.284$ marking the onset of incommensurate spin-spin correlations in the chain, and a Lifshitz point at $j_L = 0.3725$ where the excitation spectrum develops a doubly degenerate structure. The Haldane phase, characterized by the so called *string order* [13], breaks down at $j_T = 0.7446$. This transition was first interpreted [12] as a decoupling of a single Haldane chain into two subchains, and the order parameter of the large j -phase was later identified as describing two intertwined strings [11]. The transition has then a topological nature.

In this paper, we study the frustrated antiferromagnet with $S = 1$ described by Hamiltonian (1) by using the modified spin wave theory (MSWT). The MSWT was first proposed by Takahashi [14] to describe the low temperature properties of 1D and 2D Heisenberg ferromagnets. Imposing the conditions of free-energy minimum and zero magnetization, the MSWT results for $S = 1/2$ were in excellent agreement with those of Bethe-Ansatz integral equations. Later, Hirsch and Tang [15] and Takahashi [16], independently, formulated the MSWT for the two-dimensional antiferromagnetic Heisenberg model without frustration imposing the restriction of zero sublattice magnetization, analogously to what had been done for the ferromagnet. Again, the MSWT results obtained for the $S = 1/2$ antiferromagnetic 2D Heisenberg model were found to be in excellent agreement with the results of exact diagonalization [17] and renormalization-group theory [18]. It is important to remark that the MSWT results are also in agreement with the ones obtained via the Schwinger boson theory, as discussed by Arovas and Auerbach [19].

The MSWT theory was also extended to the 2D frustrated Heisenberg model [20] in order to give the phase diagram of this model. Some of us [21] applied the method to the non-frustrated one-dimensional (1D) Heisenberg model to obtain the dependence of the normalized gap, that is, the ratio between the gap at temperature T , $\Delta(T)$, to the gap at $T = 0$, Δ_0 , as a function of the normalized temperature $t = T/\Delta_0$. The results so obtained were compared to experimental data and the agreement is reasonable. More recently, Yamamoto [22] presented a slightly different version of the MSWT for the same 1D non-frustrated Heisenberg model and, again, obtained the behavior of the normalized gap as a function of t .

The theories used in references [21] and [22] are identical in the sense that they both start by writing the spin operators in terms of Bose operators obtaining a Hamiltonian involving products of two and four operators. After some manipulations, the free energy is minimized under the restriction of zero sublattice magnetization. However, the procedures used for diagonalizing the transformed Hamiltonian are different and lead to remarkably different systems of equations to be solved. The procedure adopted in [21] followed the one sug-

gested by Takahashi [16] and introduces an ideal spin-wave density matrix (SWDM) after a Bogoliubov transformation: hereafter, we will refer to this procedure as SWDM. Yamamoto [22] reduces the terms involving four operators to products of only two operators by using standard commutation relations, and, then, diagonalizes the resulting Hamiltonian imposing the coefficient of the crossed term to be zero. He calls this scheme *full diagonalization interacting modified spin-wave* and, for brevity, we will refer to it here as FD (full diagonalization).

The MSWT-FD results were used [23] to explain the nuclear magnetic relaxation in the Haldane gap antiferromagnet $\text{Ni}(\text{C}_2\text{H}_8\text{N}_2)_2\text{NO}_2(\text{ClO}_4)$ (NENP). Taking into account that the MSWT is a simple analytical theory that has successfully been applied to describe properties of low-dimensional magnets, we apply this theory to study some properties of Hamiltonian (1) and compare our results to some numerical and experimental results available in the literature. Another task of this work is to compare the different schemes used in the MSWT context. Therefore, we compare the results obtained for Hamiltonian (1), non-frustrated ($j = 0$) and frustrated, by using the SWDM and FD approaches to the MSWT.

2 The modified spin-wave theory

We start by rewriting Hamiltonian (1) assuming that the lattice is bipartite and divided in sublattices A and B : spins in sublattice A are denoted as \mathbf{T}_{2l} while those in sublattice B are \mathbf{S}_{2l+1} . Then, the model Hamiltonian is given by

$$H = J_1 \sum_l \left\{ \left[\mathbf{T}_{2l} \cdot \mathbf{S}_{2l+1} + \mathbf{S}_{2l+1} \cdot \mathbf{T}_{2l+2} \right] + j \left[\mathbf{T}_{2l} \cdot \mathbf{T}_{2l+2} + \mathbf{S}_{2l+1} \cdot \mathbf{S}_{2l+3} \right] \right\}, \quad (2)$$

where the sum runs over all l lattice sites, and $j = J_2/J_1$ is the ratio between the nnn and nn exchange interactions. Next, we define bosonic operators, a and b , for the spin deviation in each sublattice through the Dyson-Maleev transformation

$$\begin{aligned} T_{2l}^z &= S - a_{2l}^\dagger a_{2l}; & T_{2l}^- &= a_{2l}^\dagger; & T_{2l}^+ &= (2S - a_{2l}^\dagger a_{2l}) a_{2l}, \\ S_{2l+1}^z &= -S + b_{2l+1}^\dagger b_{2l+1}; & S_{2l+1}^- &= -b_{2l+1}; \\ S_{2l+1}^+ &= -b_{2l+1}^\dagger (2S - b_{2l+1}^\dagger b_{2l+1}). \end{aligned} \quad (3)$$

In the Dyson-Maleev transformation, the Hamiltonian (1) has no term higher than the fourth order, and we can construct a self-consistent theory instead of a conventional $1/S$ expansion. In terms of these bosonic operators, the Hamiltonian has now the form

$$H = E_0 + H_0 + H_1, \quad (4)$$

where $E_0 = -2J_1 N S^2 (1-j)$ and N is the number of spins in each sublattice. H_0 and H_1 represent the terms in the

Hamiltonian involving, respectively, products of two and four bosonic operators and are given by

$$H_0 = J_1 S \sum_l \left\{ 2b_{2l+1}^\dagger b_{2l+1} + 2a_{2l}^\dagger a_{2l} - (a_{2l} + a_{2l+2})b_{2l+1} - (a_{2l}^\dagger + a_{2l+2}^\dagger)b_{2l+1}^\dagger - j \left[(a_{2l+2}^\dagger - a_{2l}^\dagger)(a_{2l+2} - a_{2l}) + (b_{2l+1}^\dagger - b_{2l+3}^\dagger)(b_{2l+1} - b_{2l+3}) \right] \right\}. \quad (5)$$

and

$$H_1 = \frac{J_1}{2} \sum_l \left\{ a_{2l}^\dagger (b_{2l+1}^\dagger - a_{2l})^2 b_{2l+1} + a_{2l+2}^\dagger (b_{2l+1}^\dagger - a_{2l+2})^2 b_{2l+1} - j \left[a_{2l}^\dagger a_{2l+2}^\dagger (a_{2l} - a_{2l+2})^2 + (b_{2l+1}^\dagger - b_{2l+3}^\dagger)^2 b_{2l+1} b_{2l+3} \right] \right\}. \quad (6)$$

2.1 The SWDM scheme

Next, in the SWDM formulation for the MSWT, the ideal spin-wave density matrix

$$\rho = \exp \left(\frac{1}{T} \sum_k \epsilon_k \left\{ \alpha_k^\dagger \alpha_k + \beta_k^\dagger \beta_k \right\} \right), \quad (7)$$

is introduced with the Bogoliubov transformation

$$\begin{aligned} \alpha_k &= \cosh \theta_k a_k - \sinh \theta_k b_{-k}^\dagger \\ \beta_k^\dagger &= \cosh \theta_k b_{-k}^\dagger - \sinh \theta_k a_k. \end{aligned} \quad (8)$$

In (7), \sum_k means the sum over the half of the first Brillouin zone, and, in (8), a_k and b_{-k}^\dagger are the Fourier-transformed operators

$$\begin{aligned} a_k &= \frac{1}{\sqrt{N}} \sum_l a_{2l} e^{ik(2l-1/2)}, \\ b_{-k}^\dagger &= \frac{1}{\sqrt{N}} \sum_l b_{2l+1}^\dagger e^{-ik(2l+1/2)}, \end{aligned} \quad (9)$$

where the lattice constant a was set equal to unit.

Then, we can evaluate the terms of the density matrix obtaining for the non-null terms

$$\langle b_{2l+1}^\dagger b_{2l'+1} \rangle = f(r_{2l+1} - r_{2l'+1}) - \frac{1}{2} \delta_{l,l'}, \quad (10)$$

$$\langle a_{2l}^\dagger a_{2l'} \rangle = f(r_{2l} - r_{2l'}) - \frac{1}{2} \delta_{l,l'}, \quad (11)$$

$$\langle a_{2l} b_{2l'+1} \rangle = \langle a_{2l}^\dagger b_{2l'+1}^\dagger \rangle = g(r_{2l} - r_{2l'+1}). \quad (12)$$

where we have used the definitions,

$$\begin{aligned} f(r_{2l} - r_{2l'}) &= f(r_{2l+1} - r_{2l'+1}) \\ &= \frac{1}{2N} \sum_k e^{ik(2l-2l')} \phi_k \cosh 2\theta_k, \end{aligned} \quad (13)$$

$$g(r_{2l} - r_{2l'+1}) = \frac{1}{2N} \sum_k e^{ik(2l-2l'-1)} \phi_k \sinh 2\theta_k, \quad (14)$$

$$n_k = \langle \alpha_k^\dagger \alpha_k \rangle = \langle \beta_k^\dagger \beta_k \rangle = [\exp(\epsilon_k/T) - 1]^{-1}. \quad (15)$$

We defined $\phi_k = 2n_k + 1$. In order to obtain the energy $\mathcal{E} = \langle \mathcal{H} \rangle$, we decouple the four operator terms in H_1 according to the following example,

$$\begin{aligned} \langle a_{2l}^\dagger b_{2l+1}^\dagger b_{2l+1}^\dagger b_{2l+1} \rangle &= 2 \langle a_{2l}^\dagger b_{2l+1}^\dagger \rangle \langle b_{2l+1}^\dagger b_{2l+1} \rangle \\ &\quad + \langle a_{2l}^\dagger b_{2l+1} \rangle \langle b_{2l+1}^\dagger b_{2l+1}^\dagger \rangle. \end{aligned} \quad (16)$$

The energy \mathcal{E} is then given as

$$\mathcal{E} = -2NJ_1 \left\{ \left[S - \left(f(0) - \frac{1}{2} - g(\delta) \right) \right]^2 - j \left[S - \left(f(0) - \frac{1}{2} - f(2\delta) \right) \right]^2 \right\}, \quad (17)$$

where δ is a vector between nn sites. Following the steps in [16], we minimize the free-energy \mathcal{F} under the condition of zero site magnetization,

$$\langle T_{2l}^z \rangle = \langle S_{2l+1}^z \rangle = S + \frac{1}{2} - f(0), \quad (18)$$

obtaining

$$\tanh 2\theta_k = \frac{\eta \cos k}{1 - \Gamma \sin^2 k}, \quad (19)$$

and

$$\epsilon_k = \lambda \sqrt{(1 - \Gamma \sin^2 k)^2 - \eta^2 \cos^2 k}, \quad (20)$$

where

$$\lambda = 2J_1 g(\delta) - \mu, \quad (21)$$

$$\eta = \frac{2J_1 g(\delta)}{\lambda}, \quad (22)$$

$$\Gamma = \frac{4jJ_1 f(2\delta)}{\lambda}. \quad (23)$$

In the equations above, μ is the Lagrange multiplier used in the minimization of \mathcal{F} under restriction (18). Notice that Γ is the parameter introduced when the nnn interaction is taken into account.

The ϵ_k can be obtained after the parameters λ , Γ , and η are known. These parameters are obtained by solving the following set of self-consistent equations

$$2S + 1 = \frac{\lambda}{N} \sum_k \frac{1 - \Gamma \sin^2 k}{\epsilon_k} \coth \left(\frac{\epsilon_k}{2T} \right), \quad (24)$$

$$\frac{\eta \lambda}{2J_1} = \frac{\lambda}{2N} \sum_k \frac{\eta \cos^2 k}{\epsilon_k} \coth \left(\frac{\epsilon_k}{2T} \right), \quad (25)$$

$$\frac{\Gamma \lambda}{4J_1} = \frac{\lambda j}{2N} \sum_k \frac{\cos 2k(1 - \Gamma \sin^2 k)}{\epsilon_k} \coth \left(\frac{\epsilon_k}{2T} \right). \quad (26)$$

These equations were solved for several values of j , including $j = 0$, and the results will be discussed in Section 3. As will be discussed later, the solution of this set of equations gives $\eta < 1$ for any temperature and j value investigated. Therefore, from (20), we conclude that the MSWT theory

predicts a gap ($\epsilon_{k=0} \neq 0$) for the frustrated Heisenberg model and, in this respect, is in accordance to previous field theoretical studies [8,9]. A naive inspection of equation (20) may lead to the conclusion that the gap does not depend on the nnn interaction. It has to be remarked, however, that the values of the λ and η parameters are determined self-consistently and depend on Γ .

2.2 The FD scheme

Here, we apply the Bogoliubov and Fourier transformations defined, respectively, in (8) and (9) to Hamiltonians H_0 and H_1 . The expression obtained for H_0 is found to be

$$H_0 = E_1 + J_1 \sum_k \left\{ \omega_k^0 \left(\alpha_k^\dagger \alpha_k + \beta_k^\dagger \beta_k \right) + \gamma_k^0 \left(\alpha_k^\dagger \beta_k^\dagger + \alpha_k \beta_k \right) \right\}, \quad (27)$$

where

$$E_1 = 4J_1 SN [(1-j)\Gamma_1 - \Gamma_2 + j\Gamma_3] \quad (28)$$

$$\omega_k^0 = 2S(1 - 2j \sin^2 k) \cosh 2\theta_k - 2S \cos k \sinh 2\theta_k, \quad (29)$$

$$\gamma_k^0 = 2S \cos k \cosh 2\theta_k - 2S(1 - 2j \sin^2 k) \sinh 2\theta_k. \quad (30)$$

Notice that, here, the crossed terms like $\alpha_k^\dagger \beta_k^\dagger$ are still present (compare with Eq. (7)). E_1 represents a first correction to the ground state energy and requires the following definitions,

$$\Gamma_1 = \frac{1}{2N} \sum_k (\cosh 2\theta_k - 1), \quad (31)$$

$$\Gamma_2 = \frac{1}{2N} \sum_k \cos k \sinh 2\theta_k, \quad (32)$$

$$\Gamma_3 = \frac{1}{2N} \sum_k \cos 2k \cosh 2\theta_k. \quad (33)$$

The Wick theorem is applied to Hamiltonian H_1 leading to

$$H_1 = E_2 - J_1 \sum_k \left\{ \omega_k^1 \left(\alpha_k^\dagger \alpha_k + \beta_k^\dagger \beta_k \right) - \gamma_k^1 \left(\alpha_k^\dagger \beta_k^\dagger + \alpha_k \beta_k \right) \right\}, \quad (34)$$

where

$$E_2 = -2J_1 N (\Gamma_1 - \Gamma_2)^2 + 2jJ_1 N (\Gamma_1 - \Gamma_3)^2, \quad (35)$$

$$\omega_k^1 = 2\Gamma_1 \cosh 2\theta_k + 2\Gamma_2 \cos k \sinh 2\theta_k - 2\Gamma_1 \cos k \sinh 2\theta_k - 2\Gamma_2 \cosh 2\theta_k - 4j(\Gamma_1 - \Gamma_3) \sin^2 k \cosh 2\theta_k, \quad (36)$$

$$\gamma_k^1 = 2\Gamma_1 \sinh 2\theta_k + 2\Gamma_2 \cos k \cosh 2\theta_k - 2\Gamma_1 \cos k \cosh 2\theta_k - 2\Gamma_2 \sinh 2\theta_k - 4j(\Gamma_1 - \Gamma_3) \sin^2 k \sinh 2\theta_k. \quad (37)$$

The correction to the ground state energy due to H_1 is given by E_2 .

As before, the free energy is minimized under the constraint of zero sublattice magnetization which, here, is written as

$$\sum_l a_{2l}^\dagger a_{2l} = \sum_l b_{2l+1}^\dagger b_{2l+1} = SN \quad (38)$$

which, obviously, is equivalent to (18). A Lagrange multiplier λ_{FD} is introduced leading to a new Hamiltonian \tilde{H} given by

$$\tilde{H} = H + 2J_1(1-j)\lambda_{FD} \sum_k \left\{ 2 \sinh^2 \theta_k + \cosh 2\theta_k (\alpha_k^\dagger \alpha_k + \beta_k^\dagger \beta_k) - \sinh 2\theta_k (\alpha_k^\dagger \beta_k^\dagger + \alpha_k \beta_k) \right\} \quad (39)$$

and the whole expression for \tilde{H} is diagonalized. The diagonalization of \tilde{H} gives the expression for the θ_k parameter in the Bogoliubov transformation

$$\tanh 2\theta_k = \frac{\cos k [S + \Gamma_2 - \Gamma_1]}{\tau}, \quad (40)$$

where

$$\tau = S(1 - 2j \sin^2 k) + \lambda_{FD}(1-j) - \Gamma_1 + \Gamma_2 + 2j(\Gamma_1 - \Gamma_3) \sin^2 k.$$

Putting together the transformed expressions for H_0 and H_1 , we obtain the ground-state energy and the dispersion relation as

$$E_{GS} = E_0 + E_1 + E_2 + 4J_1 \lambda_{FD} N (1-j) \Gamma_1, \quad (41)$$

$$\omega(k) = \omega_k^0 - \omega_k^1 + 2\lambda_{FD}(1-j) \cosh 2\theta_k. \quad (42)$$

Once θ_k is given, we calculate the free energy and obtain the optimum thermal distribution function as given by (15). The Lagrange multiplier, λ_{FD} is self-consistently determined by the condition

$$2S + 1 = \frac{1}{N} \sum_k (2n_k + 1) \cosh 2\theta_k, \quad (43)$$

where n_k is the usual boson occupation number. Thus, the FD scheme requires four parameters, λ_{FD} , Γ_1 , Γ_2 , and Γ_3 to be self consistently solved.

3 Results

We start by comparing the SWDM and FD results for the non-frustrated Heisenberg model because there are more data — theoretical and experimental — available for this system. The MSWT is not a large-spin expansion method, and, thus, we can expect that it can be applied to models with small spin value. In this work, we will consider only the spin $S = 1$ case.

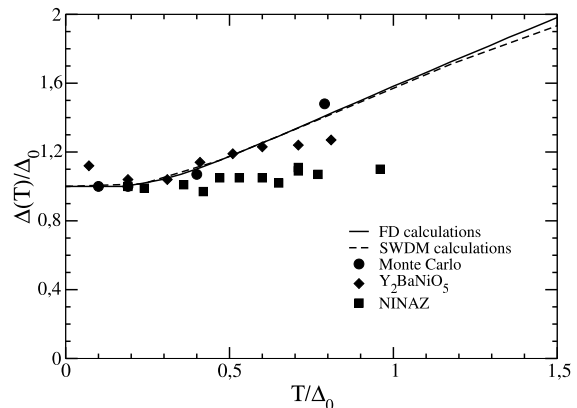
Table 1. Ground state energy, E_{GS} , and gap at zero temperature, Δ_0 .

	E_{GS}	Δ_0
SWDM	-1.49014	0.08506
FD	-1.39461	0.08523
QMC	-1.401481(4)	0.41048(6)
DMRG	-1.401484038971(4)	0.41050(2)
ED	-1.401485(2)	0.41049(2)

3.1 The non-frustrated 1D Heisenberg model

The Haldane's conjecture [1] that 1D spin-1 Heisenberg antiferromagnets should exhibit an energy gap immediately above the ground state was confirmed experimentally in quasi-1D Heisenberg antiferromagnets as the $\text{Ni}(\text{C}_2\text{H}_8\text{N}_2)_2\text{NO}_2(\text{ClO}_4)$ [24], Y_2BaNiO_5 [25], and $\text{Ni}(\text{C}_3\text{H}_{10}\text{N}_2)_2\text{N}_3(\text{ClO}_4)$ [26]. A large number of investigations — numerical, analytical and experimental — were devoted to studying the properties of the 1D Heisenberg model. Numerical methods as density matrix renormalization group, quantum Monte Carlo, and exact diagonalization (Lanczos method) have been quite useful in this study but analytical approaches still play an important role to the understanding of the peculiarities of the model. From the analytical point of view, the non-linear σ model technique [1, 27, 28] has been one of the most powerful methods to describe the low-energy structure of the model and the valence-bond description [29] of integer-spin chains was of crucial importance to the understanding of the hidden order in the Haldane massive phase. However, these analytical methods have some limitations and cannot be used, for example, to study the thermodynamic behavior of the model. In this context, as pointed out by some of us [21] and Yamamoto and Hori [22], the MSWT has been quite successful.

In Table 1, we present results for the ground-state energy, E_{GS} , as calculated via the FD and SWDM approaches and compare these data to numerical estimates obtained by using quantum Monte-Carlo [30] (QMC), density-matrix renormalization-group [31] (DMRG), and exact diagonalization [32] (ED) techniques. We observe that the FD estimate for E_{GS} is slightly closer to the numerical estimates than the SWDM. The third column of Table 1 gives the SWDM and FD estimates for the gap at zero temperature, Δ_0 : these values are very close to each other but are, both, quite smaller than the numerical estimates. We must emphasize however that, up to the present moment, no other analytical approach is able to really predict the magnitude of Δ_0 as a function of microscopic parameters. Usually, what is obtained is a set of expressions for finite temperatures involving ratios such as T/Δ_0 . Therefore, in order to compare the theoretical prediction for the temperature dependence of the gap to numerical and/or experimental data, it became usual to compare the behavior of the ratio of the gap evaluated at temperature T , $\Delta(T)$, to the zero temperature gap, Δ_0 , as a function of T/Δ_0 , as shown in Figure 1. In that figure, the continuous and dashed curves correspond, respectively, to the FD

**Fig. 1.** Normalized gap, $\Delta(T)/\Delta_0$, as a function of the normalized temperature, T/Δ_0 , for $j = 0$. The MSWT results (continuous and dashed lines) are compared to Monte Carlo data [33], and experimental data obtained for the Y_2BaNiO_5 [25] and NINAZ [26] compounds.

and SWDM results and we see that these two approaches give essentially the same result for small temperatures. For $T/\Delta_0 > 1.0$, the FD estimate becomes slightly smaller than the SWDM one. Experimental data obtained for the Y_2BaNiO_5 [25] and NINAZ [26] compounds and numerical data obtained via quantum Monte Carlo method combined with the maximum-entropy technique [33] are also shown in Figure 1.

We see that the FD and SWDM results are in good agreement with the quantum Monte Carlo data. Concerning the behavior of the theoretical curves with temperature, the comparison to the experimental data is slightly better for the Y_2BaNiO_5 compound. The data for the NINAZ compound [26] show a slower increase of $\Delta(T)/\Delta_0$ with temperature than the result predicted by the MSWT. It is important to mention that the error bars (10%) for the Y_2BaNiO_5 experimental data [25] were not included in Figure 1 and their inclusion may lead to a behavior similar to the NINAZ compound. Nevertheless, it must be remarked that the Y_2BaNiO_5 compound is a better realization [25] of the isotropic Hamiltonian (1) than the NINAZ compound because there exists a larger anisotropy in this last compound.

Although we are, here, restricting our discussion to the $S = 1$ case, it is important to mention that the MSWT predicts the zero temperature gap to decrease as $e^{-\pi S}$: this result can be obtained by using asymptotic expansions for equations (24) and (25) at $T = 0$ [19, 21]. In the case of the non-linear σ model, the renormalization group at weak coupling leads to a very similar result giving $\Delta_0 = CS^2 \exp(-\pi S)$, where C is a multiplicative factor independent of S . Then, we see that two quite different theories — MSWT and renormalization group — predict similar behavior for Δ_0 as a function of S .

We conclude this sub-section noticing that the comparison between our MSWT results and quantum Monte Carlo data allows to say that the MSWT is able to describe the behavior of the normalized gap as a function of T/Δ_0 and that the two MSWT approaches investigated

here give similar/equivalent results in despite of the remarkable difference in the set of self-consistent equations obtained in each of them. Yamamoto and Hori [23] used the FD results to interpret nuclear spin-lattice relaxation-time (T_1) measurements performed on the spin-1 quasi-1D Heisenberg antiferromagnet $\text{Ni}(\text{C}_2\text{H}_8\text{N}_2)_2\text{NO}_2(\text{ClO}_4)$ (NENP) and successfully explained the minimum of T_1^{-1} as a function of an applied field. Considering the equivalence between the FD and SWDM approaches, we can infer that similar results would be obtained by using the SWDM scheme.

3.2 The frustrated Heisenberg model

According to the classical spin-wave theory, the ground-state is Néel-like for $J_2 = 0$. The J_2 coupling introduces frustration into the problem and the Néel-state cannot be the true ground-state for large J_2 values. In the large J_2 -region, we can expect that each sublattice has some kind of spiral alignment, that is, a state that can be obtained from the Néel-state by applying a uniform twist along the chain direction. In the $S \rightarrow \infty$ limit, a classical treatment shows that the ground-state is in the Néel-phase for $4J_2 < 1$, and in a spiral phase for $4J_2 > 1$. Therefore, we cannot expect our calculations to be valid for the whole $0 \leq j \leq 1$ region because the treatment presented here departs from the boson transformation defined in (3), accounting only for small deviations from the Néel order.

The ground-state energy can be obtained from equations (17) and (41) in the SWDM and FD approaches, respectively. Our results are shown in Figure 2, where they are compared to the ones obtained numerically by Tonegawa et al. [7]. In their work, Tonegawa and co-workers applied an exact diagonalization method to investigate some ground-state properties, including the energy and the gap, for finite size systems of up to 16 sites. The extrapolation of the results to the $N \rightarrow \infty$ limit showed that the results with $N = 16$ are sufficient to discuss satisfactorily well the limiting ground-state properties. Through the analysis of the two-spin correlation function, they [7] see that this function has a commensurate character for $j \leq 0.38$ and an incommensurate character for larger j . Therefore, they restricted their calculation to the $j < 0.40$ region, as can be seen in Figure 2. Notice that our results are in very good agreement with the ones obtained in reference [7].

However, it can also be seen from Figure 2 that the FD results (triangles) shown cover only the $j < 0.25$ region while the SWDM data (circles) go up to ≈ 0.30 . This happens because we could not find a solution to the set of self-consistent equations (31–33) and (43) for $j > 0.25$ in the FD approach, and for $j > 0.30$ (Eqs. (24–26)) in the SWDM approach. We interpret this failure in finding a solution as the limit of validity for each procedure, suggesting a change in the ground-state structure, as discussed above. It is interesting to see that, when the solutions to the system of self-consistent equations can be found, the results obtained via the two approaches are almost identical (this equivalence is also observed in the calculation of the gap energy, as shown in Fig. 3).

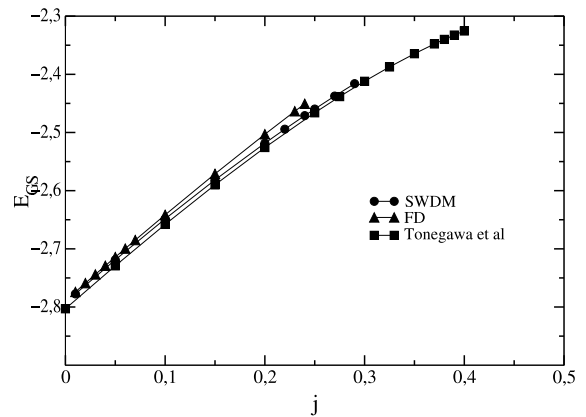


Fig. 2. Ground state energy, E_{GS} , as a function of j . The FD (triangles) and SWDM (circles) results are compared to numerical data [7] (squares) available in the literature.

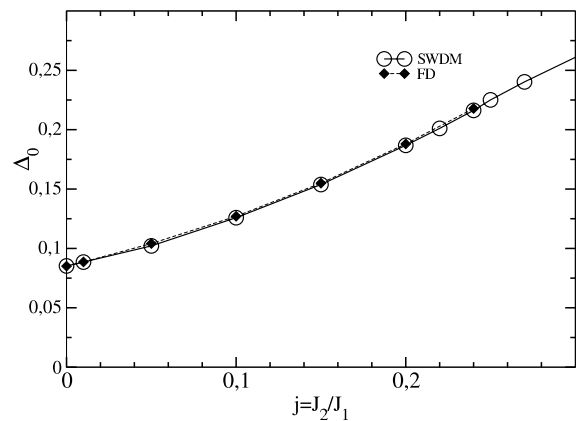


Fig. 3. Gap at zero temperature, Δ_0 , as a function of j obtained from the two MSWT approaches: FD (full losangles) and SWDM (open circles).

The gap at zero temperature, Δ_0 , as a function of the frustration parameter, j , is shown in Figure 3 where we see that, again, the FD and SWDM approaches give identical results. It can also be seen that the competition between the antiferromagnetic nn and nnn interactions stabilizes the gap since Δ_0 increases with j . This result is in qualitative agreement to the one found by Tonegawa et al. [7]. Another analytical treatment, based on the bosonization method and the self-consistent harmonic approximation [34], predicted a gap decreasing with the increase of j . However, as explained by the authors of that work, Shimaoka and Kuboki, the difference between their result and the numerical one [7] can be due to the fact that the phase diagram obtained in [34] is not accurate enough. The ground-state phase diagram and some low-energy properties of the 1D frustrated Heisenberg antiferromagnet were also investigated by Pati et al. [10] and by Kolezhuk et al. [11] by using the density matrix renormalization group method. Their results for the gap behavior as a function of j show Δ_0 increasing with the frustration parameter while j is smaller to ≈ 0.4 ; for larger j , the gap decreases up to a point, $j = 0.73$. Taking into

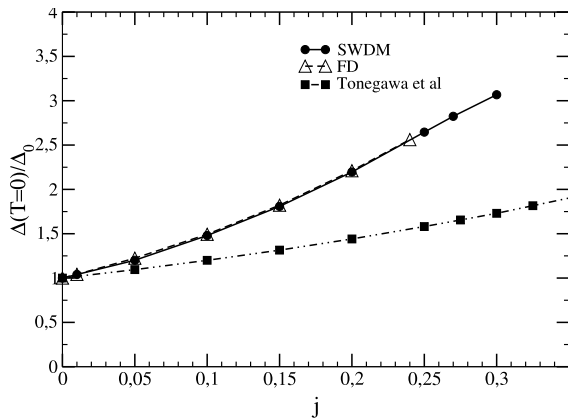


Fig. 4. Gap at zero temperature, $\Delta(T = 0)$, normalized by the gap at zero temperature for $j = 0$, Δ_0 , as a function of j . The MSWT results (open triangles \rightarrow FD, and full circles \rightarrow SWDM) are compared to the numerical results obtained by Tonegawa et al. [7] (full squares).

account that our theory is valid for small j , and that, in this region, the obtained behavior for the gap as a function of j qualitatively agrees with the numerical ones [7, 10], we conclude that the MSWT predicts the correct behavior.

In order to compare our results to the numerical ones obtained in references [7] and [10], we compare the “normalized” gap, that is, the gap obtained for a given j at zero temperature, divided by the gap for $j = 0$ at $T = 0$, Δ_0 , as a function of j in Figure 4. The normalization is necessary because the MSWT estimate for the gap is considerably smaller than the numerical estimates. As said before, no analytical procedure can predict the correct value for the gap in terms of microscopic parameters. Figure 4 shows that the MSWT results predict the ratio $\Delta(T = 0)/\Delta_0$ to increase with j much faster than the numerical results.

In Figure 5, we show the behavior of the normalized gap, for several j values, as a function of the temperature. In this figure, we present only results obtained from the SWDM scheme because we can conclude from Figure 4 that the two procedures, FD and SWDM, furnish identical results. It is interesting to notice that the $\Delta(T)/\Delta(0)$ increases with T in the same way for all j : in the range investigated, the degree of frustration, j , does not affect the dependence of the normalized gap as a function of the temperature.

The correlation function, $\langle \mathbf{S}_i \cdot \mathbf{S}_j \rangle$, is given by

$$\langle \mathbf{S}_i \cdot \mathbf{S}_j \rangle = f^2(r_i - r_j) - g^2(r_i - r_j) - \frac{1}{4} \delta_{i,j}, \quad (44)$$

where $f(r)$ and $g(r)$ are given by equations (13) and (14). The behavior of $|\langle \mathbf{S}_i \cdot \mathbf{S}_j \rangle|$, at $T = 0$, as a function of the distance between spins is shown in Figure 6: the correlation function decays faster as j increases, as expected. In fact, we verified that the decay shown in Figure 6 fits nicely to the function $\exp(-r/\xi)/\sqrt{r}$, with the parameter ξ — to be identified as the correlation length — decreasing as j increases.

The structure factor, $S(q)$, is given by the Fourier transform of (44) which for $q = 0$, the antiferromagnetic

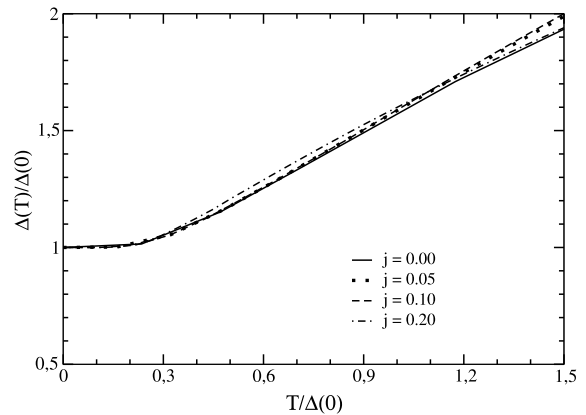


Fig. 5. Gap at temperature T , $\Delta(T)$, normalized by the value of the gap at zero temperature for each j value, $\Delta(0)$, as a function of the normalized temperature, $T/\Delta(0)$, for $j = 0.00, 0.05, 0.10$, and 0.20 .

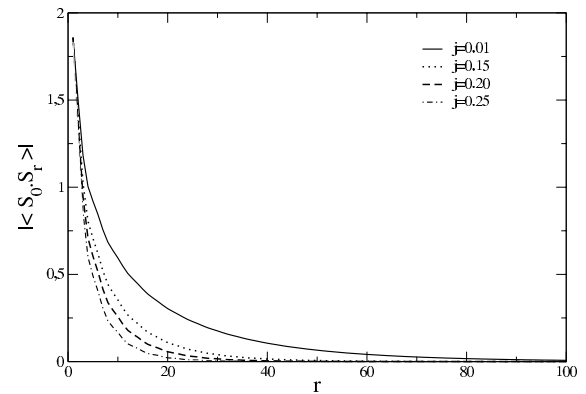


Fig. 6. Correlation function $|\langle \mathbf{S}_0 \cdot \mathbf{S}_r \rangle|$, as a function of the distance r , for several values of j .

wavevector in our treatment, is

$$S(0) = \frac{1}{N} \frac{1}{4} \sum_k \frac{(1 - \Gamma \sin^2 k)^2 + \eta^2 \cos^2 k}{(1 - \Gamma \sin^2 k)^2 - \eta^2 \cos^2 k} - \frac{1}{4}, \quad (45)$$

and, in the thermodynamic limit, is related to the mean squared staggered magnetization m by $Nm^2 = S(0)$. The solution of equations (24–26) shows that, as j varies in the range where solutions were found, η does not vary appreciably (from 0.999349 for $j = 0$ to 0.993872 for $j = 0.30$), while Γ increases approaching the value 0.50 as $j \rightarrow j_{max}$. It is easy to see that, for $\Gamma \rightarrow 0.5$, equation (45) becomes small signaling that the long range order will vanish in this limit. In fact, for $\Gamma = 0.5$, equation (24) does not have a solution, explaining why we could not solve the set of self-consistent equations for $j > j_{max}$.

4 Conclusions

In this work, we used the MSWT to investigate the ground state energy and the gap of the frustrated 1D antiferromagnetic Heisenberg model with $S = 1$. This model has attracted the interest of several numerical works that investigated the low-temperature properties and the phase-diagram of the model. There are not so many analytical

works dealing with the same model, and, for this reason, we think it is important to analyse the efficiency of a simple analytical treatment like the MSWT in describing the low-temperature behavior of the model.

Our results show that the MSWT gives good estimates of the ground-state energy and predicts a qualitatively correct behavior for the gap as a function of the frustration parameter. However, the gap is found to increase with j faster than the numerical results predict. Nevertheless, we must remember that the gap was found to *decrease* with j when the bosonization method was applied to the same model [34]. The simple MSWT can predict a correct qualitative behavior.

We compared two different procedures to implement the MSWT; here, we have referred to these approaches as FD and SWDM. The results given by each recipe are very similar except for the range of j where the solution to the set of self-consistent equations generated in each procedure can be found: in the FD scheme, $J_{max} = 0.25$ while $J_{max} = 0.30$ in the SWDM. However, we repeat here part of the short review done in the introduction: Kolezhuk, Roth and Schollwöck [12] identifies a disorder point at $j_D = 0.284$. This disorder point can arise if a system has two different low-temperature phases, e.g., an antiferromagnetically ordered phase and a spiral phase with a wave number that is, usually, incommensurate. It is also required that the two phases are linked to the disordered high-temperature phase by continuous phase transitions. A similar phase transition exists for the *classical* frustrated antiferromagnetic unidimensional Heisenberg model. For $j < j_C = 0.25$, the chain is antiferromagnetically ordered while for $j > 0.25$ there is spiral order with a wavevector given by $q(j) = \cos^{-1}(-0.25j)$. Therefore, we are tempted to suggest that the failure of the MSWT in solving the self-consistent equations it generates for $j > j_{max}$ is somehow related to this disorder point. The value of j_{max} found in the FD approach, 0.25, is quite close to the estimated j_D value [12]. Obviously, this relationship has to be investigated by analysing, for example, the behavior of the two-spin correlation function as a function of j . This investigation is in progress.

This work was partially supported by CAPES (G.M. Rocha-Filho) and CNPq (A.S.T. Pires and M.E. Gouvêa).

References

1. F.D.M. Haldane, Phys. Lett. **93A**, 464 (1983); F.D.M. Haldane, Phys. Rev. Lett. **50**, 1153 (1983)
2. S.R. White, I. Affleck, Phys. Rev. B **54**, 9862 (1996)
3. C.K. Majumdar, J. Phys. C **3**, 911 (1970)
4. B.S. Shastry, B. Sutherland, Phys. Rev. Lett. **47**, 964 (1981)
5. K. Nomura, K. Okamoto, J. Phys. A **27**, 5773 (1994); K. Nomura, K. Okamoto, J. Phys. Soc. Jpn **62**, 1123 (1993)
6. K. Okamoto, K. Nomura, Phys. Lett. A **169**, 433 (1992)
7. T. Tonegawa, M. Kaburagi, N. Ichikawa, I. Harada, J. Phys. Soc. Jpn **61**, 2890 (1992)
8. S. Rao, D. Sen, Nucl. Phys. B **424**, 547 (1994)
9. D. Allen, D. Senechal, Phys. Rev. B **51**, 6394 (1995)
10. S. Pati, R. Chitra, D. Sen, H.R. Krishnamurthy, S. Ramasesha, Europhys. Lett. **33**, 707 (1996)
11. A.K. Kolezhuk, U. Schollwock, Phys. Rev. B **65**, 100401 (2002)
12. A.K. Kolezhuk, R. Roth, U. Schollwock, Phys. Rev. Lett. **77**, 5142 (1996); A.K. Kolezhuk, R. Roth, U. Schollwock, Phys. Rev. B **55**, 8928 (1997)
13. M. den Nijs, K. Rommelse, Phys. Rev. B **40**, 4709 (1989); S.M. Girvin, D.P. Arovas, Phys. Scr. **T27**, 156 (1989); T. Kennedy, H. Tasaki, Phys. Rev. B **45**, 304 (1992)
14. M. Takahashi, Phys. Rev. Lett. **58**, 168 (1987)
15. J.E. Hirsch, S. Tang, Phys. Rev. B **40**, 4769 (1989)
16. M. Takahashi, Phys. Rev. B **40**, 2494 (1989)
17. Y. Okabe, M. Kikuchi, D.S. Nagi, Phys. Rev. Lett. **61**, 2971 (1988)
18. S. Chakravarty, B.I. Halperin, D.R. Nelson, Phys. Rev. B **39**, 2344 (1989)
19. D.P. Arovas, A. Auerbach, Phys. Rev. B **38**, 316 (1988)
20. J.H. Xu, C.S. Ting, Phys. Rev. B **42**, 6861 (1990)
21. A.S.T. Pires, M.E. Gouvêa, J. Mag. Magn. Mat. **241**, 315 (2002)
22. S. Yamamoto, H. Hori, J. Phys. Soc. Jpn **72**, 769 (2003)
23. S. Yamamoto, H. Hori, J. Phys. Soc. Jpn **73**, 822 (2004)
24. J.P. Renard, M. Verdaguer, L.P. Regnault, W.A.C. Erkelens, J. Rossät-Mognod, W.G. Stirling, Europhys. Lett. **3**, 945 (1987)
25. T. Sakaguchi, K. Kakurai, T. Yokoo, J. Akimitsu, J. Phys. Soc. Jpn **65**, 3025 (1996)
26. A. Zheludev, S.E. Nagler, S.M. Shapiro, L.K. Chou, D.R. Talham, M.W. Meisel, Phys. Rev. B **53**, 15004 (1996)
27. I. Affleck, Nucl. Phys. B **257**, 397 (1985); I. Affleck, Nucl. Phys. B **265**, 409 (1985)
28. T. Fukui, N. Kawakami, Phys. Rev. B **55**, R14709 (1997); T. Fukui, N. Kawakami, Phys. Rev. B **56**, 8799 (1997)
29. I. Affleck, T. Kennedy, E.H. Lieb, H. Tasaki, Phys. Rev. Lett. **59**, 799 (1987)
30. S. Todo, K. Kato, Phys. Rev. Lett. **87**, 047203 (2001)
31. S.R. White, D.A. Huse, Phys. Rev. B **48**, 3844 (1993)
32. O. Golinelli, Th. Jolicoeur, R. Lacaze, Phys. Rev. B **50**, 3037 (1994)
33. J. Deisz, M. Jarrell, D.L. Cox, Phys. Rev. B **48**, 10227 (1993)
34. H. Shimaoka, K. Kuboki, J. Phys. Soc. Jpn **62**, 3257 (1993)